NASA TECHNICAL NOTE

NASA TN D-5053

NASA TN D-5053

TENSILE BEHAVIOR OF BORON-FILAMENT-REINFORCED EPOXY RINGS AND BELTS

by Robert M. Baucom

Langley Research Center
Langley Station, Hampton, Va.

NATIONAL AERONAUTICS AND SPACE ADMINISTRATION • WASHINGTON, D. C. • MARCH 1969

NASA TN D-5053

TENSILE BEHAVIOR OF BORON-FILAMENT-REINFORCED EPOXY RINGS AND BELTS

By Robert M. Baucom

Langley Research Center
Langley Station, Hampton, Va.

NATIONAL AERONAUTICS AND SPACE ADMINISTRATION

For sale by the Clearinghouse for Federal Scientific and Technical Information
Springfield, Virginia 22151 – CFSTI price $3.00

TENSILE BEHAVIOR OF BORON-FILAMENT-REINFORCED EPOXY RINGS AND BELTS

By Robert M. Baucom
Langley Research Center

SUMMARY

The room-temperature tensile characteristics of boron-filament—epoxy-resin composites have been determined by utilizing ring and belt specimens. The effect of low to elevated temperatures on rings and cyclic loading on belts was also investigated. An analysis of the tensile strength of the monofilaments used for the fabrication of the composite specimens is included. In addition, a theoretical analysis of the bending stresses inherent in ring tensile testing is presented.

The average strength of the boron monofilaments before winding into the rings and belts was about 406 ksi (2800 MN/m^2). The average room temperature strength of the composites ranged from 90 ksi (620 MN/m^2) for the Naval Ordnance Laboratory (NOL) rings to 66 ksi (455 MN/m^2) for the belts. These low composite strengths are the result of two principal factors: low-filament-volume fraction in the composite, and bending stresses induced by the ring test fixtures. With these two factors considered, the filament strength in the composite NOL ring was 85 percent of the average monofilament strength.

INTRODUCTION

Filament-reinforced materials with high strength-density ratios have potential for use in advanced aerospace structures. Epoxy resins containing glass filaments oriented in selected directions have been in use for a number of years. Glass-reinforced epoxies, however, can only be considered for applications where high stiffness is not a primary design criterion.

Research and development over the past few years have led to the production of continuous lengths of boron filament which have not only strength and density comparable to glass, but also are much stiffer. By virtue of their high stiffness, boron filaments may be used with epoxy matrices in the fabrication of composites having a Young's modulus much larger than glass epoxy materials.

A general program designed to investigate the behavior of boron-filament-reinforced epoxy composites was initiated at the NASA Langley Research Center several years ago. Included in the overall program was an investigation of the tensile characteristics of unidirectional boron-filament—epoxy composite rings and belts. An evaluation of boron monofilaments (conducted prior to this program and reported in refs. 1 and 2) led to the selection of filaments produced by the halide process as the most promising for the fabrication of composites. This paper presents the results of tensile tests performed on three types of ring and belt specimens fabricated by a contractor. The effects of low and elevated temperatures and cyclic loading were also investigated. The tensile properties of the monofilaments used for the fabrication of the composite specimens were supplied by the contractor. Tensile tests of rings are frequently performed with split-D loading fixtures for ease and simplicity of testing; however, the fixed geometry of the fixture induces bending stresses in addition to the axial stress in the specimen. A theoretical analysis of the bending stresses in ring tests of this type is also presented.

The units used for the physical quantities appearing in this paper are given in both U.S. Customary Units and the International System of Units (SI). (See ref. 3.) Factors relating the two systems are given in appendix A.

MATERIALS AND SPECIMENS

The boron filaments were produced by chemical vapor plating onto a hot 0.5-mil (13 μm) tungsten wire. The filaments averaged 1.67 mils (42 μm) in diameter with a range of 1.55 to 1.80 mils (39 to 46 μm). The boron composite specimens were fabricated from a total of 290 individual boron filaments by the United Aircraft Corporation Research Laboratories under contract to NASA. All glass specimens were wound from a single lot of preimpregnated S-glass roving. The resin system for both types of filaments was Shell Epon 826 and Shell Epon Z curing agent in the ratio of 5 to 1.

The three types of boron-epoxy specimens fabricated for this evaluation are shown in figure 1. A 3.00-inch-diameter (7.6 cm) "modified NOL" ring was used instead of the standard Naval Ordnance Laboratory (NOL) rings for most of the tests to conserve boron filament material. A small number of standard NOL rings of boron-epoxy and S-glass—epoxy were tested for comparison. The third type of boron specimen was a belt (see fig. 1) which has parallel straight segments 2.00 inches (5.1 cm) long between the semicircular ends.

Each of the boron specimens was fabricated from tapes containing 20 filaments. The 0.125-inch-wide (0.32 cm) tapes were produced by gathering the filaments between two rollers, coating them with resin, and winding the resultant tape on spools between Mylar sheets. Each ring and belt specimen was wound from a single boron-epoxy tape

using approximately 0.25 lbf (1 N) of tension during winding. The composite specimens were cured for 2 hours at 90° C (363° K) and 2 hours at 150° C (423° K).

The 3.00-inch (7.6 cm) rings and belts contain 60 turns and the 5.75-inch (14.6 cm) rings contain approximately 200 turns of tape. The 5.75-inch (14.6 cm) NOL rings were finished by machining their outer surface on a lathe to a wall thickness of 0.060 inch (0.152 cm) with a rotating abrasive wheel in the tool holder. A number of short-beam shear specimens (ASTM D-2344; ref. 4) were cut from one of the 5.75-inch-diameter (14.6 cm) boron-epoxy rings and one of the S-glass—epoxy rings. These specimens were designed to determine comparative resin bonding effectiveness on the boron and S-glass filaments.

TEST PROCEDURE

Filament Tests

Room-temperature tensile tests of the boron monofilaments were performed by the contractor. A series of five tensile tests were performed on each monofilament by using specimens with a 1-inch (2.54 cm) length between grips.

Ring and Belt Tests

The tests of the boron composite specimens (table I) were conducted at the NASA Langley Research Center. The room-temperature tensile tests were performed in a 10 000-lbf capacity (44.5 kN) screw-driven testing machine. The rings and belts were placed in the appropriate split-D test fixture (see fig. 2) and loaded in tension to failure at platen separation rates of 0.01 inch and 0.02 inch (0.025 cm and 0.051 cm) per minute, respectively. The platen separation rate for the belt is more than that for the ring because of the increased overall length of the belt (zero friction being assumed).

For the low-temperature tensile tests, a cryotank was added to the testing machine. After a specimen was placed in the split-D test fixture, the cryotank was filled with coolant and positioned so that the specimen was submerged in the coolant. For the tests conducted at -110° F (194° K), a mixture of dry ice and acetone was used and for the tests at -320° F (77° K), liquid nitrogen was used. Thermocouples attached to the split-D test fixture were used to monitor the test temperature. Prior to testing, the ring was allowed to soak for 15 minutes to make certain that the temperatures of the ring and fixture were at the correct level.

The elevated-temperature tensile tests of 3.00-inch (7.6 cm) boron NOL rings were performed in the testing machine with a circulating air electric furnace attached. Temperature variation measurements in the 12-inch (30 cm) test section of the furnace indicated a maximum variation of ±5° F (3° K) at any of the elevated-temperature test levels

of 200° F (366° K), 300° F (422° K), and 400° F (477° K). The ring and test fixture were allowed to soak for a period of 10 to 12 minutes before testing. The cyclic-load tests of boron belt specimens were initiated at a frequency of 10 cpm in a screw-driven testing machine. Because this rate required long times for large numbers of cycles, this testing machine was used for cyclic loading to 10 000 cycles. If a belt survived this number of cycles, it was then transferred to a standard fatigue machine which operated at 1800 cycles per minute and cycled to failure. A thermocouple was attached to one of the series of belt specimens tested in the standard fatigue machine to check for specimen temperature change during cycling.

Shear Tests

Short-beam shear specimens approximately 0.63 inch (1.60 cm) long (ASTM D-2344, ref.4) were cut from a single 5.75-inch-diameter (14.6 cm) boron and a single S-glass NOL ring for determination of the shear strength of the filament-reinforced epoxy. Shear strength calculations were made from the loads required to delaminate the beams.

RESULTS AND DISCUSSION

Boron-Filament Tensile Tests

The failure histogram for boron filaments used in the fabrication of the 3.00-inch (7.6 cm) rings is shown in figure 3. The total number of monofilament tests represented in this figure is 490. An average filament strength of 406 ksi (2800 MN/m^2) and a standard deviation of 52 ksi (360 MN/m^2) were obtained for this group. No filament failures were recorded below 211 ksi (1450 MN/m^2) or above 551 ksi (3800 MN/m^2).

The failure histograms for the filaments used in the fabrication of the belts and the 5.75-inch (14.6 cm) rings were almost identical to that for the 3.00-inch (7.6 cm) rings. Table II gives pertinent information for the three groups of filament-failure data as determined by the contractor.

Tensile Strength of Ring and Belt Specimens

A summary of results of the boron single filament and composite room-temperature tests of the rings and belts is presented in figure 4. Results are presented for the 5.75-inch (14.6 cm) and 3.00-inch (7.6 cm) rings and 3.00-inch (7.6 cm) belts. As described in a previous section, the composite specimens were fabricated from tapes containing 20 boron monofilaments. The open vertical bars represent the range of strengths recorded for tensile tests of the monofilaments used in the fabrication of the composite. The average strength of the filaments is represented by the cross bar between the highest and lowest recorded strength values. The hatched bars represent the results

of the composite tests. The first of each pair of hatched bars for each specimen type gives the range of tensile strength for the boron-epoxy composites. The second of each pair of hatched bars represents the range of the filament strength in the composite. The composite strength for each of the specimen types appears to be very low when compared with the filament strength developed in the composite or the strength of the individual filaments used in their fabrication. This low strength can be attributed to fabrication difficulties in making the composites (resulting in low-filament volume fractions and nonuniform resin distribution) and substantial bending stresses induced in the composite by the split-D type test. The average values of individual filament, composite, and composite filament strength for each specimen type are given in table III.

As mentioned previously, split-D test fixtures (see fig. 2) were used for the ring and belt tensile tests. During loading this type of test fixture introduces bending moments (and bending stresses) in the composite between the split-D fixtures which are superimposed on the axial tensile stress. A method of analysis has been developed which relates the bending moment to the ring characteristics. The principal equations of the analysis are presented in appendix B. Discussion is presented therein of the effect on bending moment (and bending stresses) due to variations in applied axial load for ring specimens. The method of analysis indicates that the bending stresses in the boron NOL ring test are approximately 40 percent of the applied stress. The 3.00-inch-diameter (7.6 cm) boron rings had larger calculated bending stresses that were approximately 50 percent of the applied stress.

The analysis as developed in appendix B applies only to circular rings and has not been extended to belt configurations. The belt specimen was designed with a straight section which might be expected to reduce the magnitude of the bending moment. However, the average composite filament failure strength for the belts was less than that for either of the boron rings. Fabrication difficulties experienced in winding a combination of straight and curved segments and holding them in place during cure probably was more detrimental to the tensile strength than any benefits from reduced bending moment. In addition, observation of the belt specimens before testing revealed areas of nonuniform resin distribution. During loading, abrasion of filaments in an area where little resin is present could cause a reduction in the load-carrying capacity of the composite and influence scatter.

Resin distribution within the composite was checked by sectioning a few of the failed specimens and preparing them for observation in a metallograph. Cross sections of the 3.00-inch-diameter (7.6 cm) boron belt specimens are shown in figure 5(a). These photomicrographs were taken from failed specimens in an area remote from the failure zone. The upper belt contains filaments approximately 36 percent by volume, whereas the lower belt contains filaments approximately 57 percent by volume. The filament volume

percentages were determined by counting the filaments in random areas of the photomicrographs and multiplying the filament density (filaments per unit area) in the random areas by the total cross-sectional area.

Sample cross sections of various 5.75-inch-diameter (14.6 cm) rings are shown in figure 5(b). The lower three rings were wound from one tape and the upper two rings were wound from another boron tape. These rings contained from 19- to 63-percent filaments. Although the filament volume fractions for these rings varied more than those for the belts, the filaments were more evenly dispersed throughout the cross section. The large dark regions in the bottom two rings are areas of interlaminar cracking or separation that occurred during specimen failure. This separation, initiated at failure, traveled circumferentially for varying distances around the ring. The smaller rings and belts exhibited similar failure characteristics.

Filament-strength utilization (the ratio of filament strength in the composite to single filament strength) ranged from about 77 percent for the S-glass NOL rings to 85 percent for the boron NOL rings. (See table IV.) A summary of results of tests for 5.75-inch-diameter (14.6 cm) boron- and S-glass—epoxy composite rings is given in table IV. Boron-epoxy composite filament-strength utilizations of 30.5 and 68.1 percent are reported in references 5 and 6, respectively, for similar NOL ring tests. The 3.00-inch (7.6 cm) boron rings had average failure strengths that were lower than those for the 5.75-inch (14.6 cm) rings. However, with the higher bending stresses induced by the test fixture in the smaller radii rings, the filament-strength utilization averaged 68 percent.

Effect of Temperature on Strength

The effect of temperature on the tensile strength of boron-epoxy composites is shown in figure 6. The strength data are plotted as a percentage of room-temperature strength for 3.00-inch-diameter (7.6 cm) rings for the temperature range from -320° F (77° K) to 400° F (477° K). At -320° F (77° K), the composite strength was approximately 125 percent of the room-temperature strength. As the test temperature was increased, the strength of the boron-epoxy rings decreased until at 400° F (477° K) about 50 percent of the room-temperature strength was realized. Since boron filaments retain most of their room-temperature strength up to 400° F (477° K) (see ref. 1), degradation of the resin at the higher temperatures is probably the major factor in the decrease in the strength. At elevated temperatures the resin tends to lose its ability to transfer loads from one filament to another and a subsequent decrease in composite strength is realized.

Fatigue Tests

The effect of cyclic loading at 1800 cpm on boron-epoxy composite materials as determined from belt tests is shown in figure 7. Preliminary to cyclic loading, a series of seven room-temperature belt tensile tests (four for tape A and three for tape B) were performed to establish an average tensile strength for specimens wound from each tape. Additional belts wound with the same tapes were then subjected to tensile-tensile fatigue testing with an upper (σ_{max}) and lower (σ_{min}) cyclic stress limit of approximately 80 and 5 percent, respectively, of the average static tensile strength. Since the belts had two individual average base tensile strengths, the maximum stress (the upper stress limit of the cycle) in figure 7 is plotted as a percentage of the room-temperature static strength for the belts wound from each tape. Very little, if any, change in temperature was expected because of uniaxial loading parallel to the fibers and small strains in both boron fibers and epoxy resin (below yield) which tend to minimize hysteresis effects. No detectable change in the belt temperature was noted after 30 minutes of loading at 1800 cycles per minute (about 50 000 cycles).

From the series of seven room-temperature static tensile tests, it was found that there was a wide variation in the strength of the belts under static loading conditions; therefore, some scatter was expected under cyclic loading. The belt specimens wound from tape A survived from 80 to 3.5×10^6 cycles at 78 to 84 percent of the average static strength of the belts. All the belts wound from tape B were fatigue tested at 80 percent of the established average room-temperature strength. Their fatigue failures occurred from 100 to 9.5×10^6 cycles.

Since approximately the same stress levels were employed for most of the tests and the total number of survival cycles varied from about 80 to 10×10^6, the fatigue-strength data for this specimen type exhibit considerable scatter due to scatter in static strength.

Interlaminar Shear Strength

The results of short-beam shear tests on boron- and S-glass-reinforced epoxy are presented in table V. The average interlaminar shear strength for the boron- and S-glass—epoxy tests was 7981 and 8908 psi (55.0 and 61.5 kN/m^2), respectively. For both materials there was little scatter in the test results; therefore the shear strength was very uniform in each case. Since low interlaminar shear strengths are a measure of poor filament-resin bonding and the shear strengths recorded for both types of composites were good for the resin system used, it appears that good filament-resin bonding was obtained.

CONCLUSIONS

The tensile characteristics of boron-filament epoxy resin composites have been determined by utilizing ring and belt specimens as part of a general investigation of boron-filament properties and the strength of boron composites. The following conclusions may be drawn from the results:

1. The general scatter in all the tensile results appears mainly to be due to lack of uniformity in resin content in the specimens.

2. The average strength of the boron monofilaments before winding into rings and belts was approximately 406 ksi (2800 MN/m^2). After winding into 5.75-inch (14.6 cm) rings, 3.00-inch (7.6 cm) rings, and 3.00-inch (7.6 cm) belts, the average composite filament strengths were 247, 183, and 159 ksi (1700, 1260, and 1090 MN/m^2), respectively.

3. A theoretical analysis of the bending present in split-D tensile tests showed that the maximum bending stress calculated for boron and S-glass NOL rings at failure was approximately 40 and 20 percent, respectively, of the applied average stress level. For 3.00-inch-diameter (7.6 cm) boron rings, the maximum calculated bending stress was approximately 50 percent of the applied stress.

4. The results of tensile tests of 5.75-inch (14.6 cm) rings indicate that a high utilization of the monofilament strength can be achieved in boron composites as well as in glass composites when appropriate consideration is given to filament volume fraction and induced bending stress.

5. As the test temperature was increased from -320° F (77° K) to 400° F (477° K), the boron-composite ring strength decreased from 125 to 50 percent of the average room-temperature strength. The deterioration of ring strength at elevated temperatures was attributed to degradation of the resin matrix.

6. A large degree of scatter in cycles to failure was observed in the results of tensile-tensile cyclic loading of the 3.00-inch (7.6 cm) belt specimens between stress limits of approximately 5 and 80 percent of the base tensile strength. The belts survived from 80 to 9.5×10^6 cycles when cycled at a rate of 1800 per minute.

Langley Research Center,
National Aeronautics and Space Administration,
Langley Station, Hampton, Va., January 6, 1969,
129-03-09-03-23.

APPENDIX A

CONVERSION OF U.S. CUSTOMARY UNITS TO SI UNITS

The conversion factors required for units used herein are drawn from reference 3 and presented in the following table:

Physical quantity	U.S. Customary Unit	Conversion factor (*)	SI Unit
Force	lbf	4.448	newtons (N)
Length	in.	0.0254	meter (m)
Stress	$\text{ksi} = \frac{1000 \text{ lbf}}{\text{in}^2}$	6.895×10^6	newtons per square meter (N/m^2)
Temperature	^{o}F	5/9 (F + 459.67)	degrees Kelvin (^{o}K)

*Multiply value given in U.S. Customary Units by conversion factor to obtain equivalent value in SI units.

Prefixes to indicate multiple of units are as follows:

Prefix	Multiple
giga (G)	10^9
mega (M)	10^6
kilo (k)	10^3
centi (c)	10^{-2}
micro (μ)	10^{-6}

APPENDIX B

THEORETICAL ANALYSIS OF BENDING STRESSES

As discussed previously, the split-D test fixture used for the ring tests introduces bending moments (and bending stresses) in the composite which are superimposed on the axial tensile stress. The method of analysis developed below relates the maximum bending moment developed in the ring to such characteristics of the ring as dimensions, materials, and applied stress.

The following definitions of symbols apply to the composite bending-moment equations.

A	cross-sectional area
E	Young's modulus of filamentary composite loaded parallel to filaments
G	shear modulus in plane of laminates
I	moment of inertia of cross section about neutral axis
l	half-length of ring segment assumed to be free of contact with split-D fixture, measured from center line of separation between split-D fixtures
M	bending moment
$M_{\text{¢}}$	bending moment in composite at center line of separation between split-D fixtures
M_O	bending moment in section of ring in contact with split-D fixture
P	applied tensile load on ring cross section
R	initial radius of ring measured to center of specimen thickness
t	thickness
x,y	distances along X- and Y-axes, respectively
α	shear correction factor

APPENDIX B

δ stand-off distance measured perpendicular to loading direction from point of tangency of ring with split-D fixture to center of ring at center line between split-D fixtures

θ slope of elastically deformed ring segment l, measured at point of contact with split-D fixture with respect to specimen load axis or the slope of split-D fixture at point of contact with ring specimen l, measured with respect to loading direction

ρ radius of curvature

σ_b bending stress

Under ideal test conditions (that is, internal pressurization), an NOL type ring will be in a state of uniaxial tension and will stretch to a larger circular radius $R + \Delta R$

$$\Delta R = \frac{PR}{AE}$$

But in order for the ring to be loaded by the split-D test fixture with radius $\left(R - \frac{t}{2}\right)$, the expanded ring must be bent back to its original radius R by action of bending moment M_O over most of the fixture.

$$M_O = M_1 - M_2$$

where M_1 is the moment required to bend initially straight beam to curvature $\frac{1}{\rho} = \frac{1}{R}$ and M_2 is the moment required to bend initially straight beam to curvature $\frac{1}{\rho} = \frac{1}{R + \Delta R}$. Therefore

$$M_O = \frac{EI}{R} - \frac{EI}{R + \Delta R}$$

or

$$M_O = \frac{EI\,\Delta R}{R(R + \Delta R)}$$

Substituting for ΔR in the preceding equation yields

$$M_O = \frac{IP}{A\left(R + \frac{PR}{AE}\right)} \tag{1}$$

Since for most engineering material, $\Delta R = \frac{PR}{AE}$ and is very small compared with R, it can be neglected as a first approximation for M_O; that is,

$$M_O \approx \frac{P}{A}\frac{I}{R}$$

APPENDIX B

The extreme outer fiber bending stress in the ring is

$$\sigma_b \approx \frac{M(t/2)}{I} \approx \frac{(P/A)(t/2)}{I}$$

and for typical rings with $t = 0.06$ inch and $R = 3.00$ inches

$$\sigma_b \approx 0.01 \frac{P}{A}$$

Thus the bending stress due to M_o acting on most of the ring is negligible compared with the gross section tensile stress.

Consider the small portion of the ring that spans the separation between the split-D fixtures. (See fig. 8.) From membrane theory this part of the beam may lift off the split-D fixture for a short distance when loaded. Tensile stretching of the ring under load P is taken up as a separation of the split-D fixtures, Δ, or $\Delta/2$ to the center line

$$\frac{\Delta}{2} = \frac{\pi PR}{2AE}$$

The general bending moment for the part of the beam shown in figure 8 is

$$M = M_o - P(\delta - y) \tag{2}$$

The total curvature of a ring subjected to bending and shear deflections (ref. 7) is given by

$$\frac{d^2y}{dx^2} = \frac{M}{EI} + \frac{\alpha\, d^2M}{AG\, dx^2} + \frac{1}{R} \tag{3}$$

Since $M = M_o - P(\delta - y)$ and $\alpha = 1.2$ for rectangular cross sections,

$$\frac{d^2y}{dx^2} = \frac{M_o - P(\delta - y)}{EI} + \frac{1.2P\, d^2y}{AG\, dx^2} + \frac{1}{R} \tag{4}$$

and equation (4) reduces to

$$\frac{d^2y}{dx^2} - \frac{P}{EI\left(1 - \frac{1.2P}{AG}\right)} y = \frac{1}{1 - \frac{1.2P}{AG}} \left(\frac{P\delta - M_o}{EI} + \frac{1}{R}\right)$$

Let

$$k^2 = \frac{P}{EI\left(1 - \frac{1.2P}{AG}\right)}$$

then

$$\frac{d^2y}{dx^2} - k^2y = \frac{1}{1 - \frac{1.2P}{AG}} \left(\frac{P\delta - M_o}{EI} + \frac{1}{R}\right)$$

Solving for y yields

$$y = \frac{EI}{P\left(1 - \frac{1.2P}{AG}\right)}\left(\frac{P\delta - M_O}{EI} + \frac{1}{R}\right)(1 - \cosh kx) \tag{5}$$

The slope at the point of tangency of the ring to the split-D fixture is

$$\theta = \tan^{-1}\left\{\left(\frac{M_O}{P} - \delta + \frac{EI}{R}\right)\sqrt{\frac{P}{EI\left(1 - \frac{1.2P}{AG}\right)}}\sinh\left[\frac{l}{\sqrt{\frac{EI\left(1 - \frac{1.2P}{AG}\right)}{P}}}\right]\right\} \tag{6}$$

and δ is found from equation (5) to be

$$\delta = \left(\frac{M_O}{P} + \frac{EI}{PR}\right)\left\{1 - \frac{1}{\cosh\left[\frac{l}{\sqrt{\frac{EI\left(1 - \frac{1.2P}{AG}\right)}{P}}}\right]}\right\} \tag{7}$$

Combining equations (6) and (7) yields

$$\theta = \tan^{-1}\left\{\left(\frac{M_O}{P} + \frac{EI}{PR}\right)\sqrt{\frac{P}{EI\left(1 - \frac{1.2P}{AG}\right)}}\tanh\left[\frac{l}{\sqrt{\frac{EI\left(1 - \frac{1.2P}{AG}\right)}{P}}}\right]\right\} \tag{8}$$

Because of tangency of the ring with the split-D fixture at $x = l$, the angle θ can also be represented by trigonometry as

$$\theta = \sin^{-1}\left(\frac{l}{R} - \frac{\pi P}{2AE}\right) \tag{9}$$

At the center line of separation of the split-D fixtures (y = 0),

$$M_{\text{¢}} = M_O - P\delta$$

$$M_{\text{¢}} = -\frac{EI}{R} + \left(M_O + \frac{EI}{R}\right)\left\{\frac{1}{\cosh\left[\frac{l}{\sqrt{\frac{EI\left(1 - \frac{1.2P}{AG}\right)}{P}}}\right]}\right\}$$

Calculations have been made for the maximum bending moment and related maximum bending stress at failure in the boron and S-glass rings tested in this investigation and the results are presented in figure 9. The bending stress is assumed to vary linearly across the ring thickness and is superimposed on the experimental gross section axial stress; only the maximum extreme fiber bending stress is shown in figure 9 added to the

experimental axial failure stress. For the S-glass rings the bending stress is 18 percent of the axial stress, but for the boron the bending stress is 40 and 51 percent of the axial stresses for the 5.75- and 3.00-inch-diameter (14.6 and 7.6 cm) rings, respectively. At any given applied stress level the calculations indicate that the boron rings have approximately three times the bending stress in similar S-glass rings.

REFERENCES

1. Herring, Harvey W.: Selected Mechanical and Physical Properties of Boron Filaments. NASA TN D-3202, 1966.

2. Herring, Harvey W.; and Krishna, V. Gopala: Shear Moduli of Boron Filaments. NASA TM X-1246, 1966.

3. Comm. on Metric Pract.: ASTM Metric Practice Guide. NBS Handbook 102, U.S. Dep. Com., Mar. 10, 1967.

4. Anon.: Plastics – Specifications; Methods of Testing Pipe, Film, Reinforced and Cellular Plastics. Pt. 26 of 1967 Book of ASTM Standards With Related Material. Amer. Soc. Testing Mater., c.1967.

5. Jaffe, E. H.: Boron Fibers in Composites. Proceedings 21st Annual Technical Conference, Sec. 8-C, Soc. Plast. Ind., Inc., Feb. 1966.

6. Morris, E. E.; and Alfring, R. J.: Cryogenic Boron-Filament-Wound Containment Vessels. Aerojet 3475(Contract NAS 3-10282), Aerojet-General Corp., Nov. 1967.

7. Bleich, Friedrich: Buckling Strength of Metal Structures. McGraw-Hill Book Co., Inc., 1952.

TABLE I.- SUMMARY OF BORON COMPOSITE TENSILE AND SHEAR TESTS

Test type	Temperature		Reinforcement	Number of tests
	^{o}F	^{o}K		
Standard NOL ring				
Tensile	78	299	S-glass	5
Beam shear	78	299	S-glass	11
Tensile	78	299	Boron	5
Beam shear	78	299	Boron	10
Modified NOL ring				
Tensile	-320	77	Boron	3
Tensile	-110	194	Boron	3
Tensile	78	299	Boron	18
Tensile	200	366	Boron	4
Tensile	300	422	Boron	4
Tensile	400	477	Boron	4
Belt				
Tensile	78	299	Boron	22
Cyclic	78	299	Boron	9

TABLE II.- BORON FILAMENT TENSILE PROPERTIES

Specimen type	Filament tests	Filament strength						Standard deviation	
		Average		Maximum		Minimum			
		ksi	MN/m^2	ksi	MN/m^2	ksi	MN/m^2	ksi	MN/m^2
NOL ring	255	404	2780	527	3640	211	1450	52	360
Modified NOL ring	490	406	2800	551	3800	211	1450	52	360
Belt	705	409	2810	548	3780	211	1450	52	360

TABLE III.- BORON FILAMENT AND COMPOSITE PROPERTIES

Specimen type	Filament strength		Average filament volume fraction, percent	Composite* filament strength		Composite strength	
	ksi	MN/m^2		ksi	MN/m^2	ksi	MN/m^2
NOL ring	404	2780	36	247	1700	90	620
Modified NOL ring	406	2800	39	183	1260	72	500
Belt	409	2810	41	159	1090	66	455

*Composite ultimate load divided by cross-sectional area of boron filaments.

TABLE IV.- TENSILE STRENGTH OF 5.75-INCH-DIAMETER (14.6 cm) COMPOSITE RINGS

	Composite tensile strength		Composite filament tensile strength		Filament* strength utilization, percent
	ksi	MN/m^2	ksi	MN/m^2	
			Boron		
	81	557	262	1810	
	146	1008	294	2030	
	115	794	188	1990	
	62	429	312	2150	
	47	322	178	1230	
Average	90	622	247	1700	85
			S-glass		
	265	1827	451	3110	
	254	1819	433	2985	
	186	1281	317	2185	
	276	1902	470	3240	
	258	1778	440	3030	
Average	248	1721	422	2910	77

*Filament strength utilization is the ratio of filament strength in the composite to monofilament strength. Tabulated composite filament strengths are increased 40 to 18 percent to correct for induced bending, and monofilament strengths of 404 and 650 ksi (2780 and 4500 MN/m^2) are used in the calculation of filament strength utilization for the boron and S-glass rings, respectively.

TABLE V.- SHEAR STRENGTH OF S-GLASS AND BORON REINFORCED EPOXY COMPOSITES

	Shear strength of Boron		Shear strength of S-glass	
	psi	kN/m^2	psi	kN/m^2
	8020	55 300	8490	58 400
	8210	56 500	8620	59 400
	8050	55 500	9380	64 600
	7960	54 900	9210	63 400
	7880	54 300	9220	63 500
	7830	54 000	8660	59 600
	8070	55 600	8970	61 800
	8030	55 400	8700	59 800
	7780	53 600	8880	61 200
	7990	55 000	8990	61 900
			8870	61 200
Average	7980	55 000	8910	61 500

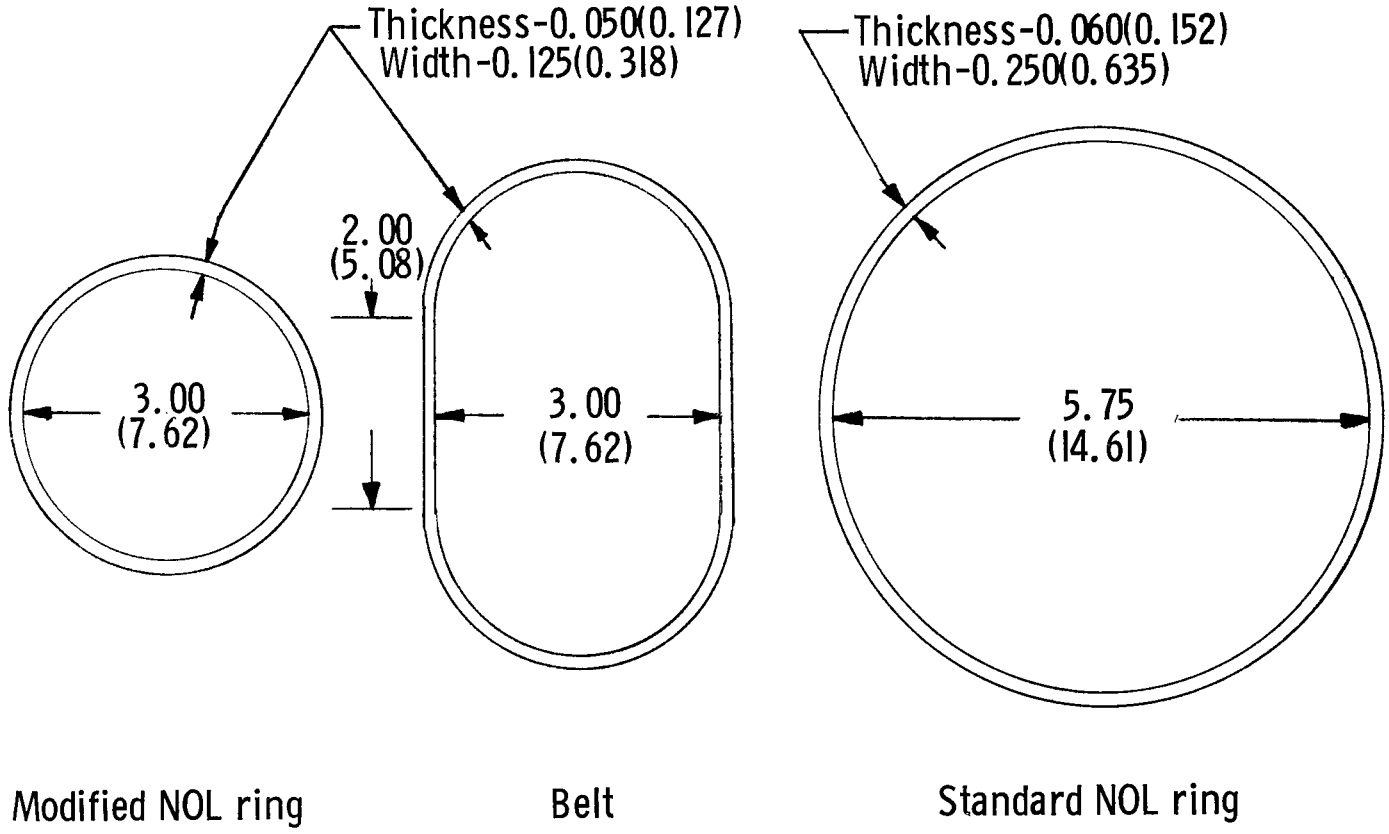

Figure 1.- Boron test specimen configurations. Dimensions are in inches (centimeters).

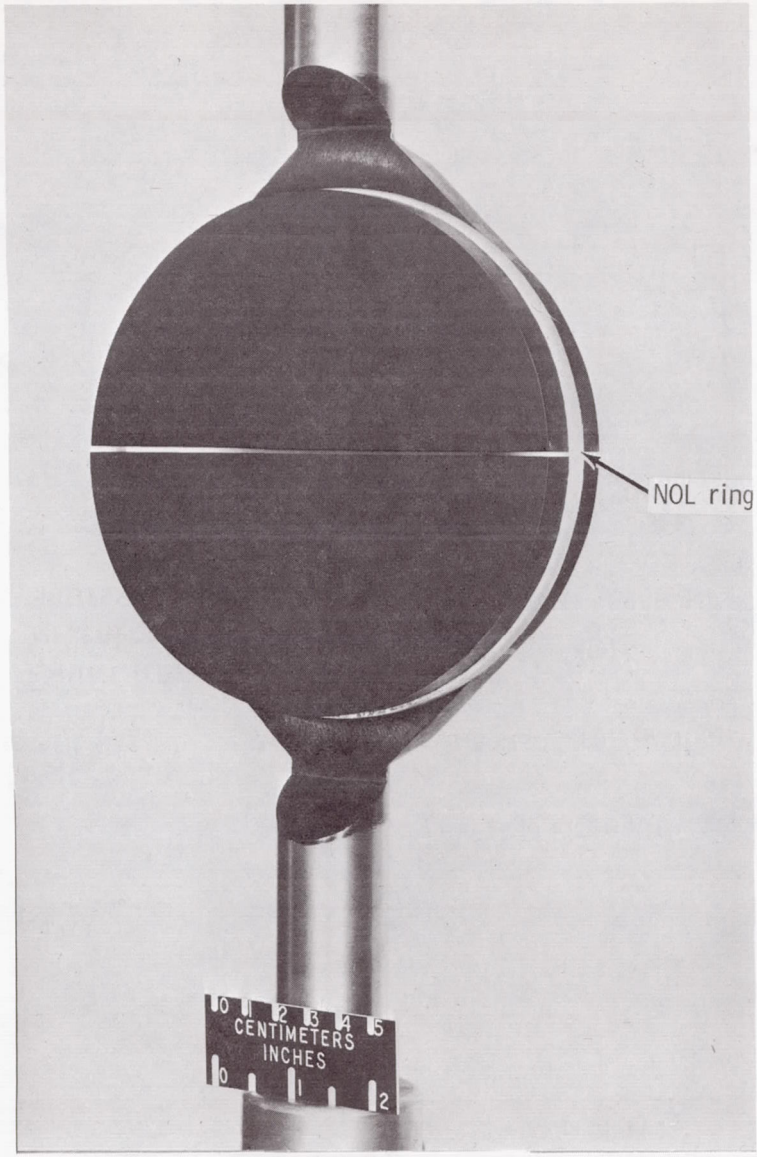

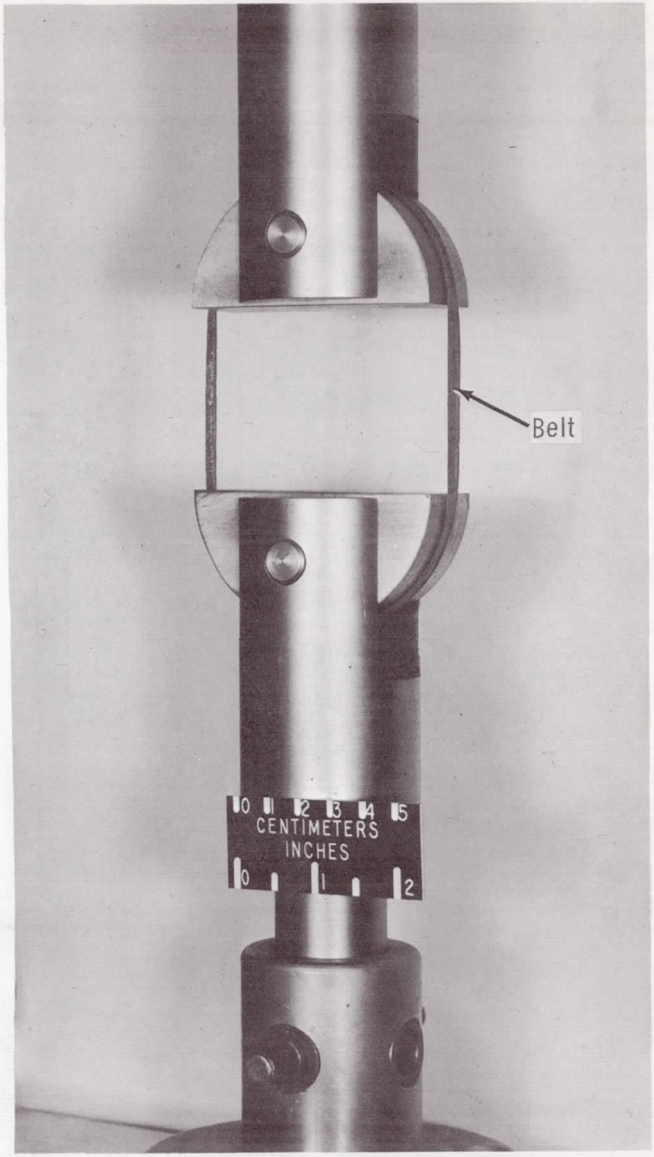

Figure 2.- Boron NOL ring and belt specimens positioned in split-D test fixtures. L-68-10,094

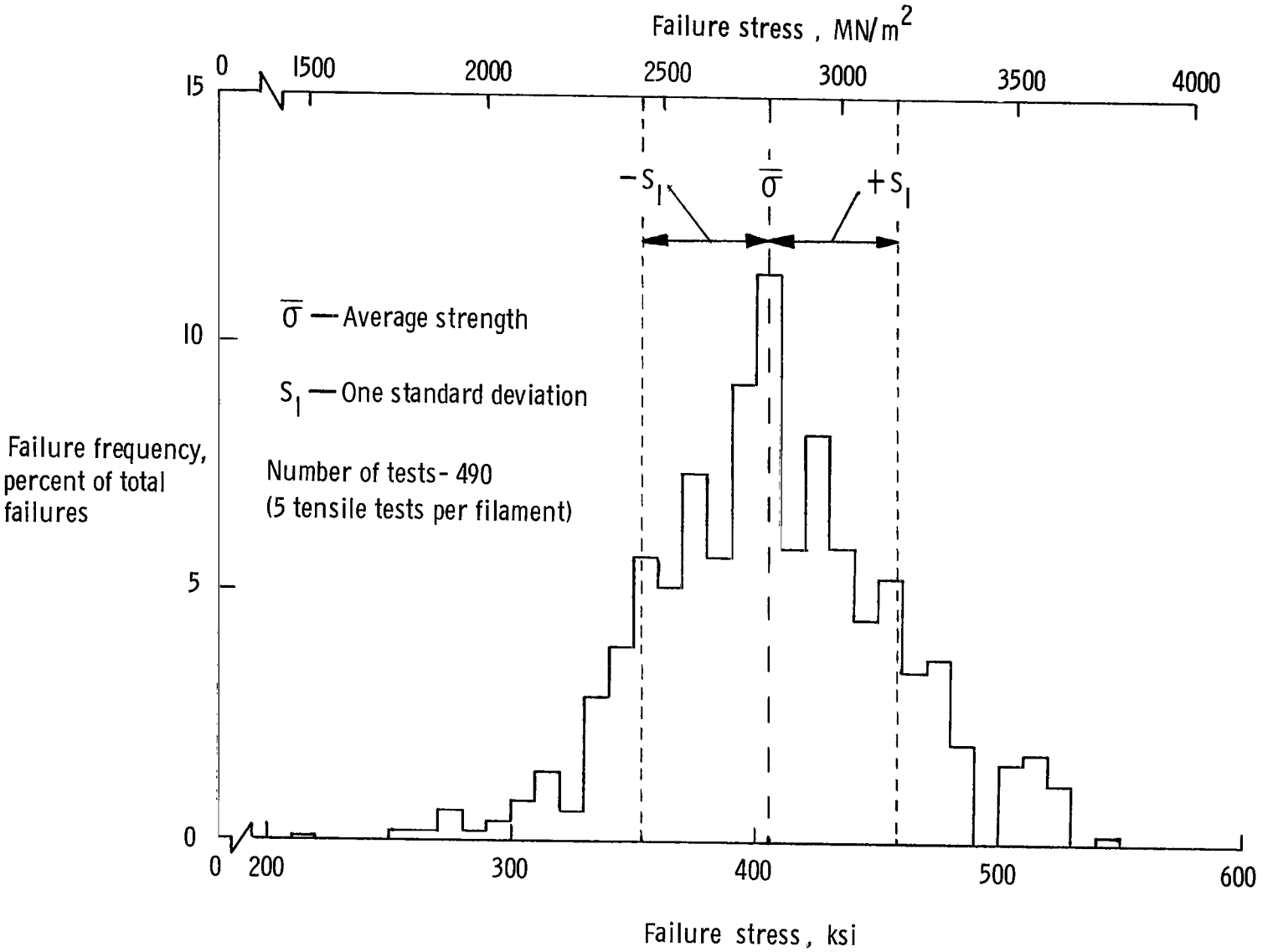

Figure 3.- Failure histogram for boron filaments used in the fabrication of 3.00-inch (7.6 cm) rings.

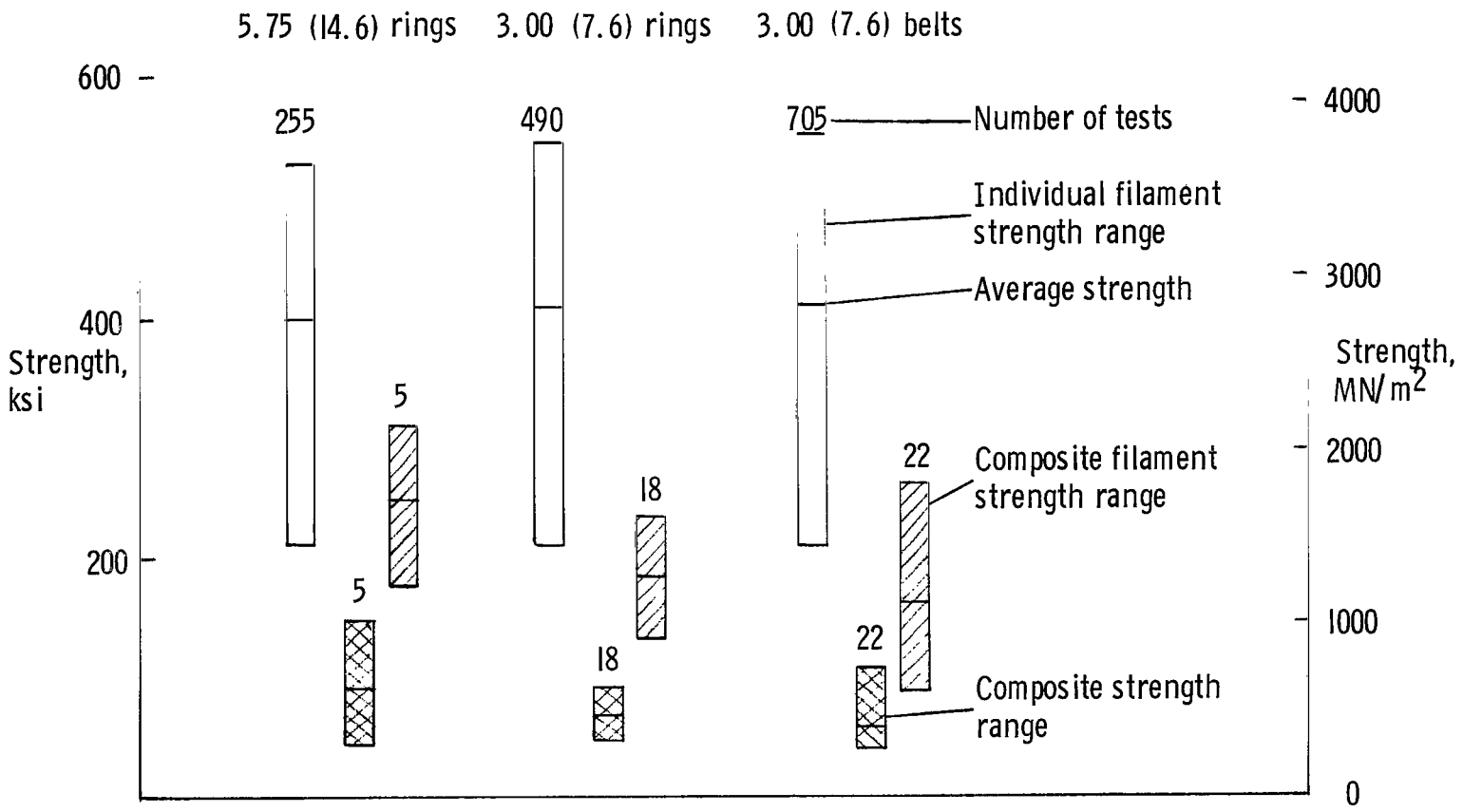

Figure 4.- Room-temperature strengths of boron (filaments) and composites.

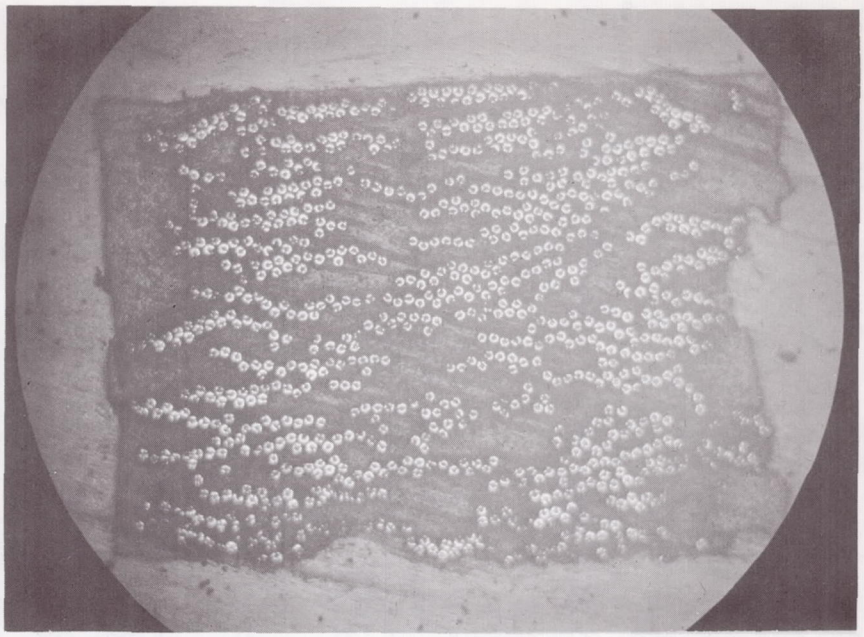

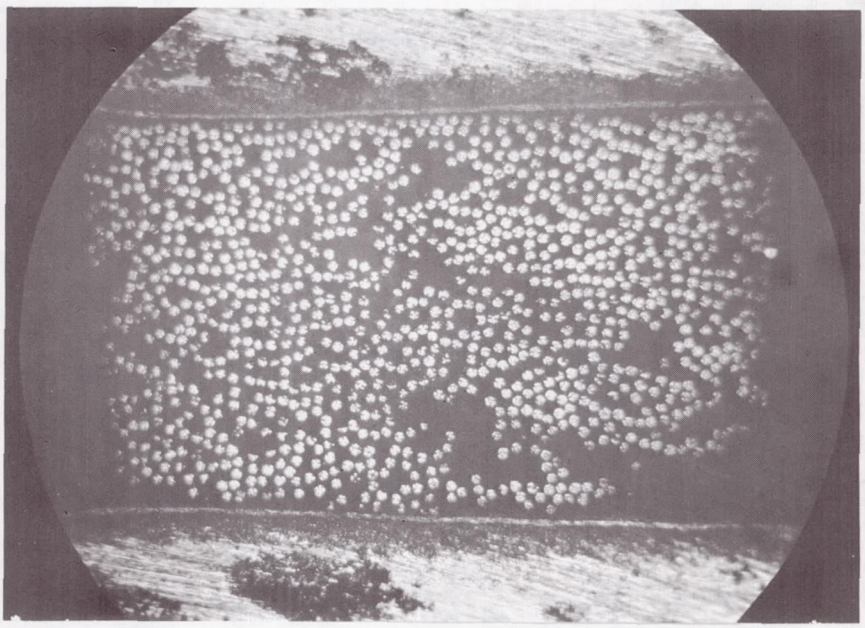

(a) Belt specimens.

Figure 5.- Typical cross sections of boron specimens. L-68-10,095

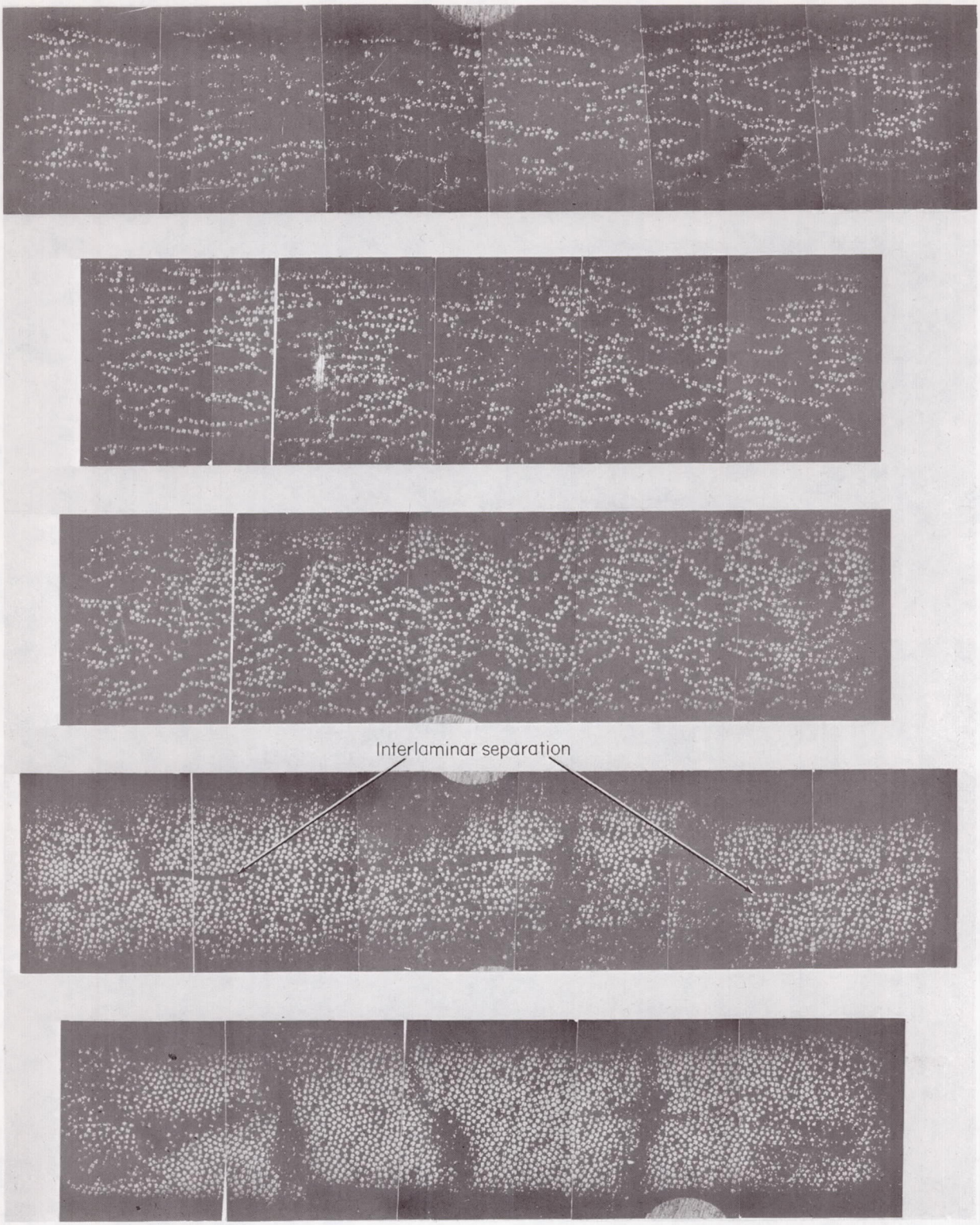

(b) 5.75-in. (14.61 cm) diameter NOL rings.

Figure 5.- Concluded.

L-68-10,096

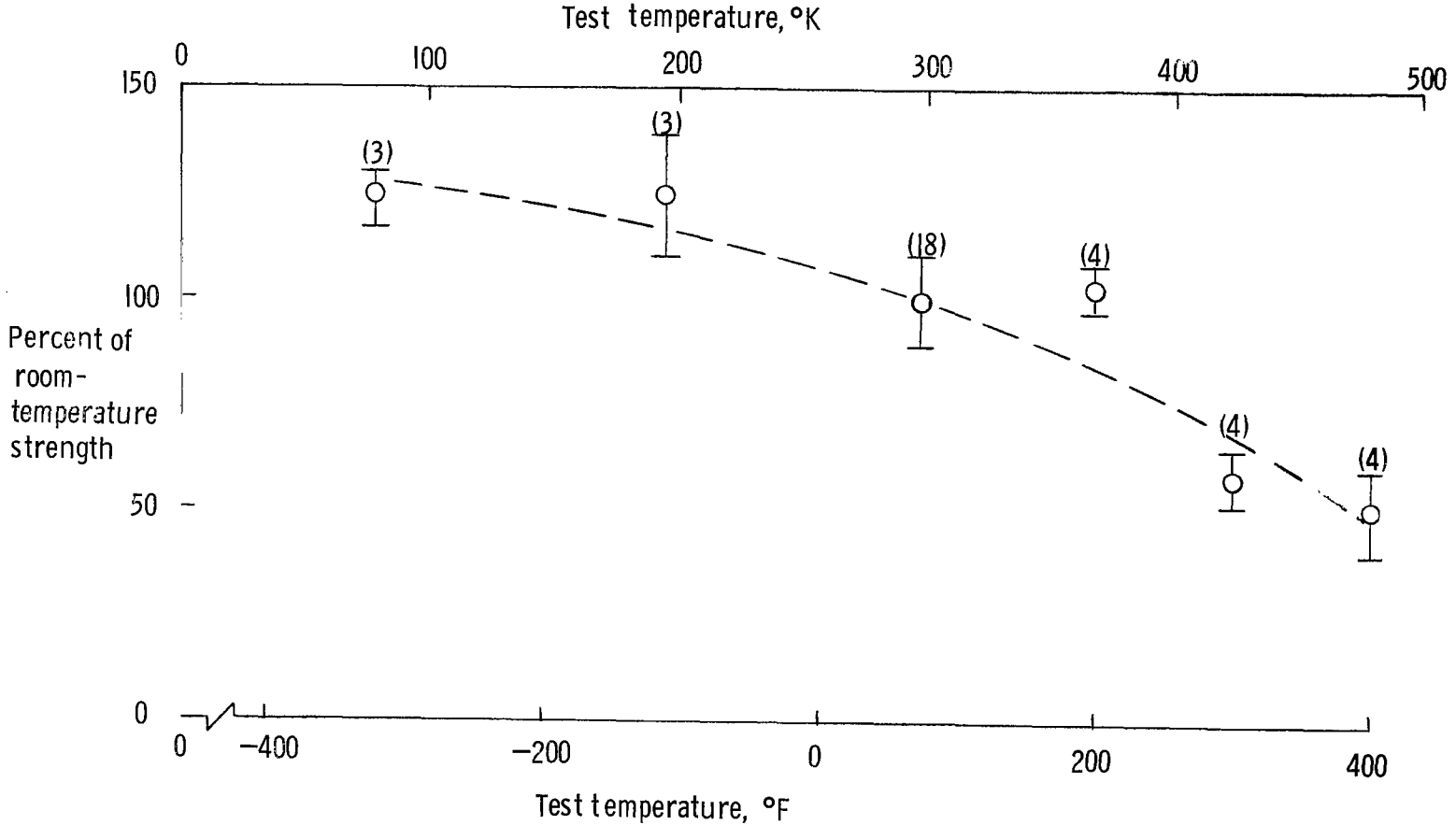

Figure 6.- Effect of temperature on the tensile strength of boron-epoxy ring specimens. Numbers in ( ) denote number of tests.

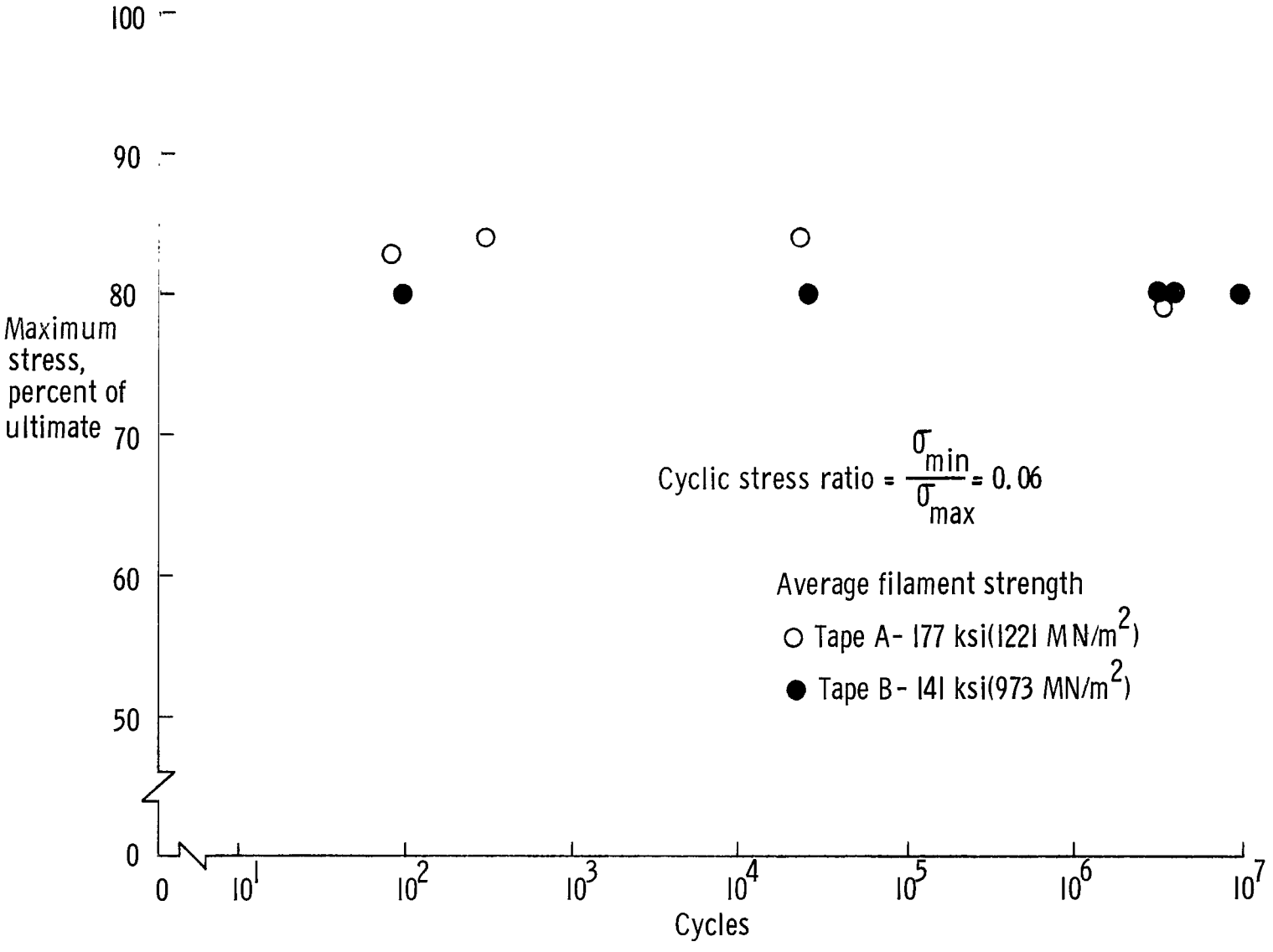

Figure 7.- Fatigue strength of boron belts.

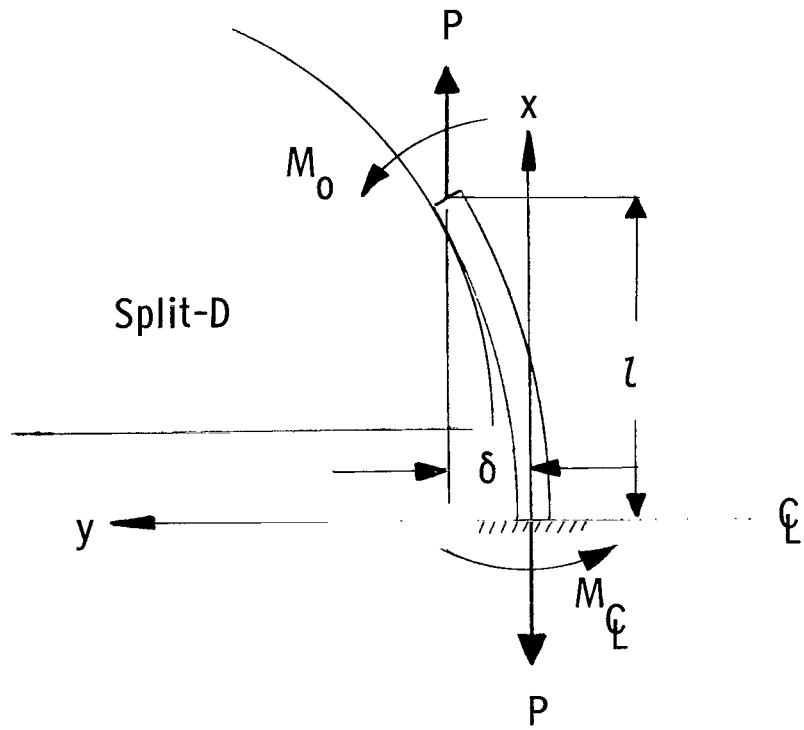

Figure 8.- Schematic diagram of portion of ring segment that lifts off split-D under load.

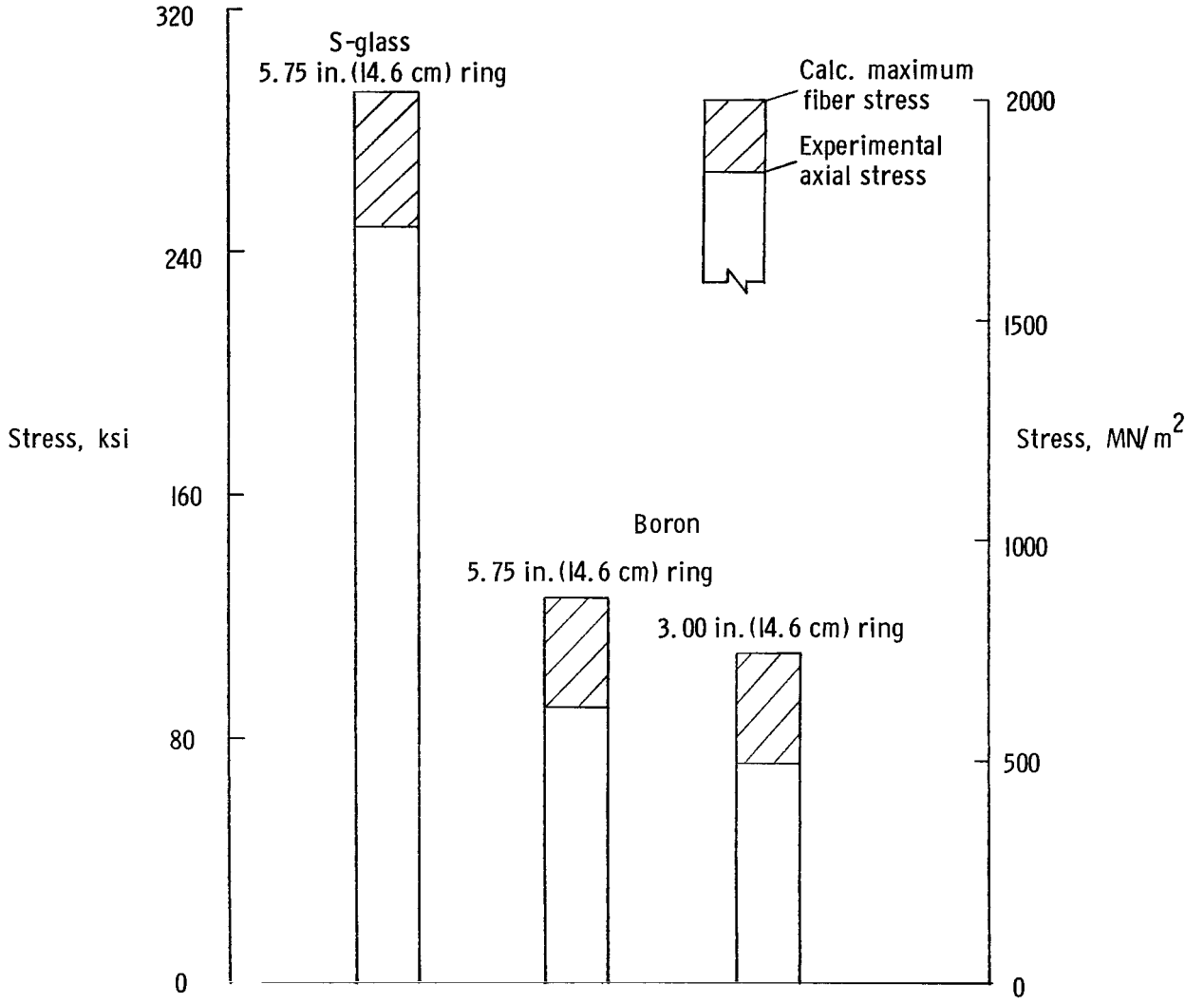

Figure 9.- Average axial and calculated bending stress levels for NOL and modified NOL rings.